Accepted Manuscript

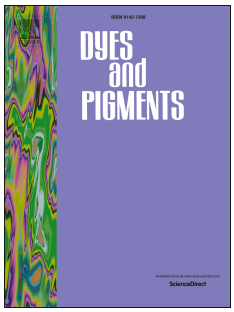

Simultaneous visualization of cysteine/homocysteine and glutathione in living cells and *Daphnia magna* via dual-signaling fluorescent chemosensor

Mingwang Yang, Jiangli Fan, Wen Sun, Jianjun Du, Saran Long, Xiaojun Peng

PII: S0143-7208(19)30775-2

DOI: https://doi.org/10.1016/j.dyepig.2019.04.056

Reference: DYPI 7511

To appear in: *Dyes and Pigments*

Received Date: 9 April 2019

Revised Date: 22 April 2019

Accepted Date: 23 April 2019

Please cite this article as: Yang M, Fan J, Sun W, Du J, Long S, Peng X, Simultaneous visualization of cysteine/homocysteine and glutathione in living cells and *Daphnia magna* via dual-signaling fluorescent chemosensor, *Dyes and Pigments* (2019), doi: https://doi.org/10.1016/j.dyepig.2019.04.056.

Graphical abstract

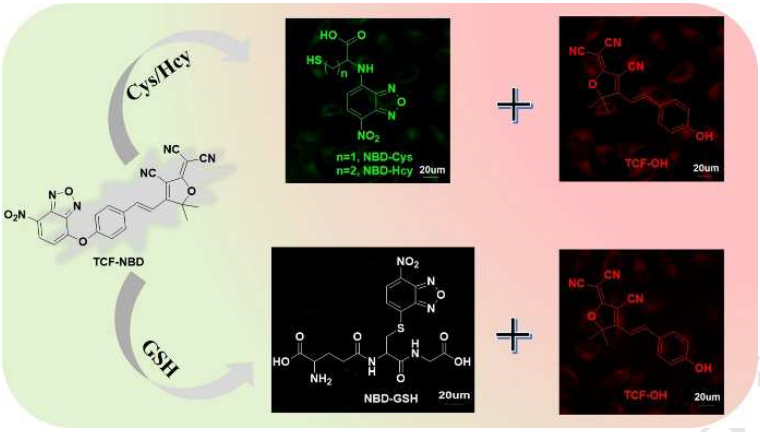

A fluorescent probe for simultaneous discrimination of cysteine/homocysteine and glutathione was developed to visualize biothiols in living cells and *Daphnia magna*.

Simultaneous visualization of cysteine/homocysteine and glutathione in living cells and *Daphnia magna* via dual-signaling fluorescent chemosensor

Mingwang Yang[1], Jiangli Fan*[1,2], Wen Sun[1,2], Jianjun Du[1,2], Saran Long[1,2], Xiaojun Peng[1,2]

[1]State Key Laboratory of Fine Chemicals, Dalian University of Technology, 2 Linggong Road, Dalian, 116024, P.R. China.

[2]Research Institute of Dalian University of Technology in Shenzhen, Gaoxin South fourth Road, Nanshan District, Shenzhen 518057, China

***Corresponding Author:**

Jiangli Fan, Email: fanjl@dlut.edu.cn

Abstract

Biological thiols, including cysteine (Cys), homocysteine (Hcy) and glutathione (GSH), play crucial roles in living organisms, such as maintaining the cellular redox equilibrium, and are closely related to many diseases. The development of efficient fluorescent probes that can diacritically detect biothiols with similar reactivity are of great desirable for the study of biological processes. The conventional single-emission fluorescent probes may be disturbed by surrounding environment and biological systems, which is greatly lose the accuracy of its detection. Herein, we have constructed a fluorescent probe (**TCF-NBD**) by connecting two fluorophores with a biothiol-reactive linker, which has two separated emissions at 547 nm and 610 nm via different excitations (470 nm and 570 nm, respectively), for simultaneously fast

detecting Cys/Hcy and GSH with high selectivity and sensitivity. Furthermore, the probe **TCF-NBD** exhibits low cytotoxicity and was successfully applied to visualize intracellular biothiols in living cells and *Daphnia magna* by fluorescence imaging. We believe that **TCF-NBD** can be a powerful tool for conducting the research of thiol-related diseases.

Keywords: Fluorescent probe; Biothiols; Bioimaging; Separated emissions; *Daphnia magna.*

1. Introduction

Intracellular biothiols, such as cysteine (Cys), homocysteine (Hcy) and glutathione (GSH), play essential roles in many physiological processes, especially in maintaining cellular redox homeostasis [1-3]. Much studies have shown that abnormal levels of cellular thiols are closely related with a various of diseases including liver damage, Parkinson's disease, leucocyte loss, psoriasis, cardiovascular diseases, Alzheimer's and hair depigmentation [4-9]. Consequently, the effective detection of biothiols is significant for intensive understanding the relationship between diseases and biothiols and evaluating the disease progression.

Fluorometry have attracted more attention due to its high sensitivity, fast-response, good biocompatibility, high spatiotemporal resolution and simple operation [10-18], which are conducive to be applied in biological systems. According, various of fluorescence probes based on the strong nucleophilicity or the high binding affinity towards metal ions of the biothiols have been developed to visualize the thiols in vitro and vivo [19-32]. Most of the optical probes involve specific reactions between thiols

and probes including Michael addition, cyclization or cleavage reaction [33-56]. Yao and co-workers reported a coumarin-benzothiazolium fluorescent probe (**BCC**) for selectively detect Cys, Hcy and GSH in DMSO/PBS (pH 7.4, 10 mM, v/v 6:4) [54]. Sun et al identified a commercial compound, 2,3,5,6-tetrafluoroterephthalonitrile (**4F-2CN**), which was used for simultaneously distinguish Cys, Hcy and GSH with the addition of CTAB and a detection time up to 2h [55] (**Table S1**). However, many of them also suffer from various of deficiencies, such as longer response time, the inability to distinguish between Cys/Hcy and GSH, the need for surfactants or higher ration of organic solvent (**Table S1**). Since the concentration of Cys (30-200 μM) and Hcy (5-12 μM) are much lower than GSH (1-10 mM) in cells as well as the similar structures and reaction activities of Cys/Hcy and GSH, it would be highly desirable to construct fluorescent sensor that could simultaneous distinguish Cys/Hcy and GSH with few interferences and a rapid response time, which is helpful to understand their generation and metabolism mechanisms [57,58].

The single-emission fluorescent probes may be disturbed by surrounding environment and biological systems, but, by contrast, the two-emissions channels fluorescent probes could effectively avoid these interferences due to its good self-calibration of two build-in excitation and emission wavelengths [59,60]. In this work, we develop a fluorescent probe for simultaneously detecting Cys/Hcy and GSH with different emissions via two independent excitation wavelengths, as shown in **Scheme 1**. The probe **TCF-NBD** consists of two parts: a dicyanomethylenedifuran-based fluorophore (**TCF-OH**) and 7-Nitrobenzofurazan

(**NBD**), connecting by an ether linker which serves as the recognitive group for Cys/Hcy and GSH and allow the probe exhibits two separated emission signals upon reaction with biothiols. The probe **NR-HNO** is non-fluorescent state due to the intramolecular electron transfer (ICT) blocked quenching [61-63]. Since Cys/Hcy would induce the occurrence of intramolecular rearrangement cascade reaction [64-67], in the presence of Cys/Hcy, there were two separated different fluorescence emissions, including **NBD** moiety in 547 nm and **TCF-OH** in 610 nm with two independent excitations (470 nm and 570 nm, separately). Due to the lack of a proximal amine group, however, GSH was unable to induce intramolecular rearrangement reaction, which resulting that only one emission of **TCF-OH** (610 nm) was observed in the presence of GSH [61, 63]. The probe **TCF-NBD** exhibited high sensitivity and selectivity to distinguish between Cys/Hcy and GSH toward others amino acids by dual fluorescence signals in vitro and vivo and a rapid response time (about four minutes). Moreover, the probe is low cytotoxicity and was successfully applied to visualize intracellular Cys/Hcy and GSH in living HeLa cells and *Daphnia magna* by fluorescence imaging.

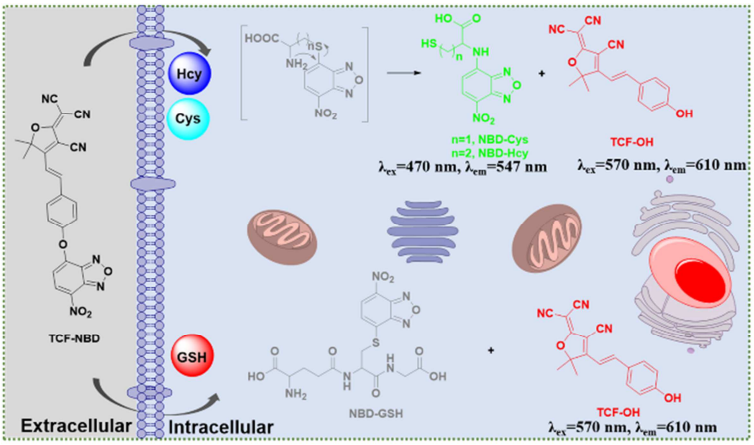

Scheme 1 Chemical structure and response mechanism of **TCF-NBD** for Cys/Hcy and GSH

2. Experimental section

2.1. Materials and instruments

All chemicals and solvents were purchased from commercial suppliers and used without further purification unless otherwise stated. The solvents were purified by traditional methods before used. 4-chloro-7-nitrobenzo[c], [1,2,5] oxadiazole was purchased from TCI chemical. Silica gel (200-300 mesh) used for flash column chromatography was purchased from Qingdao Haiyang Chemical Co., Ltd. ^{1}HNMR and ^{13}CNMR spectra were determined by 400 MHz and 100 MHz using Bruker NMR spectrometers. Chemical shifts (δ) were expressed as parts per million (ppm, in $CDCl_3$ or DMSO). Meanwhile, high-resolution mass spectrometry was achieved with ESI-TOF instrument. The absorption spectra and fluorescence spectra were measured on a PerkinElmer Lambda 35 UV−vis spectrophotometer and Agilent Technologies CARY Eclipse fluorescence spectrophotometer respectively. The pH values of detection solutions were determined with a precise pH-meter pHS-3C. MTT assays

experiments were conducted on the Varioskan LUX Multimode Microplate Reader. The Olympus FV 1000 confocal microscopy was used for live HeLa cells fluorescence imaging

2.2. The preparation of TCF-NBD

Compound 1: NaOEt (0.9 g, 13 mmol) was added to EtOH (10 mL) solution which include 3-hydroxy-3-methyl-2-butanone (9 g, 88 mmol) and malonitrile (12 g, 181 mmol) and then stirred for 1 h. After that, 30 mL EtOH was added and the mixture was then refluxed for 1 h, which was then cooled in refrigerator. The solid precipitate was filtered and washed with minimal amount of cold EtOH, affording the compound **1** as off-white crystalline solid (8.8 g, 44 mmol, 50.0 %). ^{1}H NMR (400 MHz, DMSO-d_6) δ (ppm): 2.37 (s, 3H), 1.60 (s, 6H). MS (ESI-TOF): calculated for $C_{11}H_8N_3O^-$, $[M-H]^-$, m/z, 198.07, found: 198.42.

TCF-OH: The 4-hydroxybenzaldehyde (0.122 g, 1 mmol) and compound **1** (0.3 g, 1.15 mmol) were mixed in EtOH (10 mL), then two drops of piperidine were added to the mixture. The reaction was conducted in the microwave reactor for 20 min at 100^{o}C, which was then cooled to room temperature. After he solvent was removed, the residue was purified by column chromatography with CH_2Cl_2: MeOH (50:1) to afford the desire product as a deep brown solid (0.197 g, yield 65.0%).^{1}H NMR (400 MHz, DMSO-d_6) δ (ppm): 10.61 (s, 1H), 7.90 (d, J = 16.2 Hz, 2H), 7.80 (d, J = 8.5 Hz, 2H), 7.02 (d, J = 16.3 Hz, 1H), 6.90 (d, J = 8.6 Hz, 2H), 1.77 (s, 6H). MS (ESI-TOF): calculated for $C_{18}H_{12}N_3O_2^-$, $[M-H]^-$, m/z, 302.09, found: 302.36.

TCF-NBD: The Et_3N (0.056 mL, 0.4 mmol) was added to a mixture of **TCF-OH** (60.4 mg, 0.2 mmol) and NBD-Cl (80 mg, 0.4 mmol) in 5 mL of DMF. The mixture was stirred overnight at 25 ^oC under argon atmosphere. After the reaction completed, 50 mL of water was added to the mixture and extracted with dichloromethane for three times, dried over anhydrous Na_2SO_4. After he solvent was removed, the residue was purified by silica gel column chromatography with CH_2Cl_2: MeOH (20:1) as the eluent to afford the desired product as yellow solid (59 mg, 63.3%). ^1H NMR (400 MHz, DMSO-d_6) δ (ppm): 8.68 (d, J = 8.4 Hz, 1H), 8.14 (d, J = 8.5 Hz, 2H), 7.98 (d, J = 16.3 Hz, 1H), 7.55 (d, J = 8.5 Hz, 2H), 7.29 (d, J = 16.8 Hz, 1H), 6.93 (d, J = 8.6 Hz, 1H), 1.82 (s, 1H). ^{13}C NMR (101 MHz, DMSO-d_6) δ (ppm): 177.52, 175.46, 156.36, 152.50, 146.17, 145.92, 144.93, 135.71, 133.26, 132.40, 131.46, 121.77, 116.48, 113.08, 112.24, 111.82, 111.22, 100.46, 99.97, 55.21, 25.55. HRMS (ESI-TOF): calculated for $C_{24}H_{13}N_6O_5^-$, [M-H]$^-$, m/z, 465.0953, found: 465.0959.

2.3. Spectral studies

The probe **TCF-NBD** was dissolved in DMSO to form the stock solution at a concentration of 2 mM. The stock solutions (10 mM) of Cys, Hcy and GSH were prepared in ultrapure water. The following solutions (50 mM) were prepared in deionized water: amino acids (His, Asp, Val, Phe, Tyr, Ala, Ser, Leu, Arg, Pro, Thr, Trp, Lys), and inorganic salts ($NaHCO_3$, $NaClO_4$, NaOAc, $AgNO_3$, NaSCN, $PdCl_2$, $MgCl_2$, NaF, KBr, KI, Na_2SO_4, Na_2SO_3, Na_2S, $FeCl_3$, $CaCl_2$, $ZnCl_2$, $CuCl_2$). For the spectral test, the probe stock solution was diluted to 10 μM in 10 mM PBS buffer

(containing 10% DMF) solutions and then the various of analytes were added and reacted at 37 °C for 10 min. Unless otherwise stated, the excitation wavelength is 470 nm and 570 nm for all measurements.

2.4. Determination of detection limits

The calibration curve was determined by the relationship between the specific wavelength fluorescence intensity and the analyte concentration (Cys, Hcy or GSH). The probe detection limit was calculated using the equation: Detection limit = 3σ/k. Where σ is the standard deviation of the blank sample (n=10), k is the slop between the fluorescence intensity versus the concentrations of biothiols.

2.5. Cell culture and cell viability assay

Human cervical cancer cells (HeLa) were purchased form Institute of Basic Medical Sciences (IBMS) of the Chinese Academy of Medical Sciences. HeLa cells were cultured in 90% Dulbecco's Modified Eagle Medium (DMEM) including with 10% FBS and 1% antibiotics (100 U/mL penicillin and 100 μg/mL streptomycin) in an atmosphere of 37°C and 5% CO_2. The MTT method was employed to evaluate the cytotoxicity of probe **TCF-NBD**. Before experiments, HeLa cells at a density of 1×10^4 cells/well were seeded into 96-well plates and cultured for 24 h. Then the fresh culture with different concentrations of **TCF-NBD** (0-30 μM) (n = 6) were used to replace the previous media, and further incubation for 24 h. After that, 10 μL of MTT (5 mg/mL in PBS) was added into per well and incubated for another 4 h. Finally, 100 μL of DMSO was then added to dissolve formazan. The absorbance at 490 nm was

measured, and the cell viability (%) was calculated according to the following equation: Viability (%) = [OD490 (sample) - OD490 (blank)] / [OD490 (control) - OD490 (blank)] × 100

2.6. Cell imaging experiments

One day before imaging, the HeLa cells were replanted separately on glass-bottomed dishes and incubated for 24h. In the first control experiment, the cells were pretreated with or without NEM (500 μM) at 37 °C for 30 min, then washing cells with PBS, the cells were further incubated with the probe **TCF-NBD** (10 μM) at 37°C for 30 min before imaging. In the second experiments, the HeLa cells were pretreated with NEM (500 μM) at 37°C for 30 min and washed three times with PBS, then the cells were further incubated with 100 μM Cys, Hcy or GSH respectively for 30 min, then incubated with the probe **TCF-NBD** (10 μM) at 37 °C for 30 min before imaging.

2.7. Fluorescence imaging experiment in *Daphnia magna*

The *Daphnia magna* (age < 72 h) were cultured in clean non-chlorinated tap water under cool-white light (14 h)-dark (10 h) photoperiod. The animals were pretreated with or without 500 μM NEM for 30 min, and then incubated with 10 μM **TCF-NBD** for another 30 min, followed by washing twice with PBS before imaging.

3. Results and discussion

3.1. Synthesis of TCF-NBD

TCF-NBD was readily synthesized by coupling **TCF-OH** with

4-chloro-7-nitro-1,2,3-benzoxadiazole in the presence of Et_3N at room temperature (**Scheme S1**). The target compound was well characterized by ^1H NMR, ^{13}C NMR, HR-MS (**Figs. S6-S12**).

3.2. Spectral response of TCF-NBD to Cys/Hcy and GSH

The optical spectra evaluation of probe and its reaction with Cys, Hcy and GSH were initially measured in PBS (10 mM, pH 7.4, 10% DMF). As shown in **Fig. 1A**, the probe **TCF-NBD** shows the obvious absorption peak at 400 nm. When the Cys and Hcy were added respectively, significant absorption peak appeared at both around 470 nm and 570 nm. While in case of GSH, the main absorption peak appeared only at 570 nm.

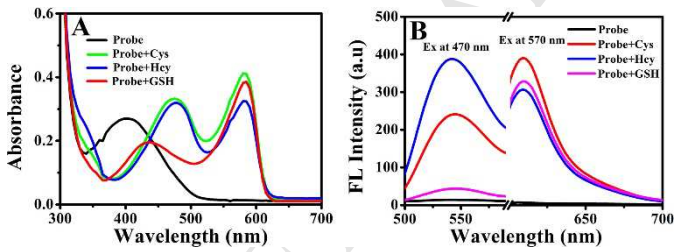

Fig.1 The absorption spectra (A) and fluorescence spectra (B) changes of probe **TCF-NBD** (10 μM) prior and after addition of Cys, Hcy, GSH (100 μM each) in PBS (10 mM, pH 7.4, 10% DMF) at 37°C for 10 min. For fluorescence measurements, λ_{ex} =470 nm and 570 nm for **NBD** moiety and **TCF–OH** moiety respectively.

Due to the presence of intramolecular electron transfer (ICT) blocked quenching, the probe is non-fluorescent when the excitation wavelength is 470 nm or 570 nm. The fluorescence responses of the probe **TCF-NBD** (10 μM) to different concentration of Cys/Hcy or GSH are summarized in **Figs. 2A-I**. Upon increasing the concentrations

of Cys or Hcy, both the fluorescence intensity at 547 nm and 610 nm gradually increased when excitation wavelengths were 470 nm and 570 nm, respectively (**Figs. 2A-F**). The fluorescence intensity at 547 nm and 610 nm reached plateau when 100 μM analytes were added (**Fig. S1**). And the detection limit of Cys and Hcy were calculated to be 0.015 μM and 0.034 μM respectively (**Table S2**). In the case of GSH, the fluorescence intensity at 610 nm increased gradually and the fluorescence emission signal at 547 nm did not change significantly (**Figs. 2G-I**). The detection limit for GSH were determined to be 0.030 μM (**Table S2**). In order to make a deeper understanding of the reaction mechanism, we monitored the reaction process of the probe **TCF-NBD** and biothiols by HRMS. The new peak appeared at m/z=302.0937 $[M]^-$ was attributed to **TCH-OH** and another peak appear at m/z=283.0150 $[M]^-$ was assigned to **TCF-Cys** (**Fig. S4**); similarly, in **Fig. S5**, the peak at m/z= 469.0783 was the product **TCF-GSH**. Thus, the probe **TCF-NBD** can simultaneous differentiate Cys/Hcy and GSH with different excitation wavelengths.

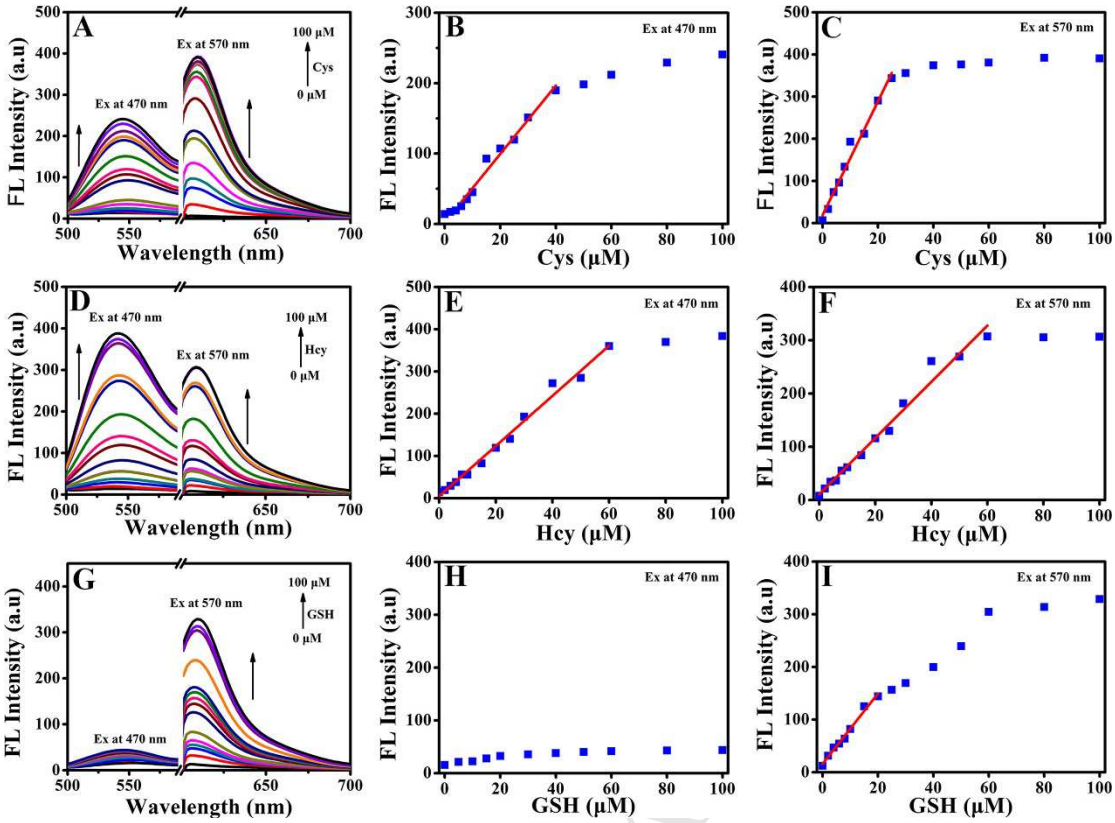

Fig. 2 Fluorescence spectra of TCF-NBD (10 μM) upon addition of varied concentration of Cys (A), Hcy (D) and GSH (G) respectively in PBS (10 mM, pH 7.4, 10% DMF). Fluorescence intensity changes at 547 nm as a function of concentrations of Cys (B), Hcy (E) and GSH (H) respectively and at 610 nm as a function of concentrations of Cys (C), Hcy (F) and GSH (I) respectively. For fluorescence measurements, λ_{ex} =470 nm and 570 nm for **NBD** moiety and **TCF–OH** moiety respectively.

3.3. Time-dependent and pH-dependent fluorescence changes of probe TCF-NBD

We then investigated the time-dependent fluorescence response of the probe **TCF-NBD** in the presence of 100 μM Cys/Hcy and GSH (**Fig. 3**). Upon addition of

Cys and Hcy, the fluorescence intensity of probe at 547 nm and 610 nm increased rapidly and reached plateau within 10 min. When GSH was added, the fluorescence intensity at 610 nm could reach its strongest after 10 min of reaction, while there was almost no significant fluorescence change at 547 nm with the extended response time. Meanwhile, the effect of pH from pH 5.0-9.0 on the fluorescence detection of Cys/Hcy and GSH were carried out. As shown in **Fig. S2**, in the absence of thiols, the probe **TCF-NBD** shows little fluorescence change but displays significant fluorescence enhancement at 610 nm in the pH range from 6.0-8.0 with 100 μM Cys, Hcy and GSH, respectively. Meanwhile, Cys/Hcy can also increase the fluorescence

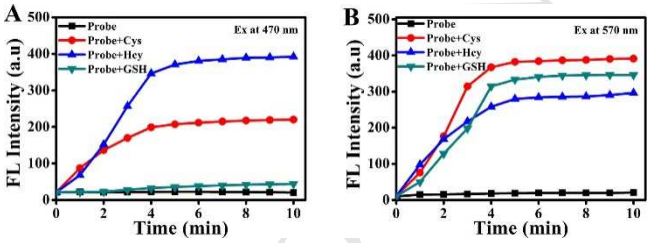

intensity at 547 nm in the pH range of 7.0-9.0. These data show that the probe is capable of detecting biothiol under physiological conditions.

Fig. 3 Time-dependent changes of fluorescence intensity at 547 nm (A) and 610 nm (B) of probe **TCF-NBD** (10 μM) upon addition of 100 μM Cys, Hcy, GSH in PBS (10 mM, pH 7.4, 10% DMF). λ_{ex} =470 nm and 570 nm.

3.4. Selectivity of probe TCF-NBD

High selectivity is a necessary and crucial indicator for the application of the fluorescent probe to biological system. We then used various analytes, such as amino acids (His, Asp, Val, Phe, Tyr, Ala, Ser, Leu, Arg, Pro, Thr, Trp, Lys,) and ions (HCO_3^-, ClO_4^-, OAc^-, NO_3^-, SCN^-, F^-, Cl^-, Br^-, I^-, SO_3^{2-}, SO_4^{2-}, S^{2-}, Pd^{2+}, Mg^{2+}, Fe^{3+}, Ca^{2+}, Zn^{2+},

Cu^{2+}) and others (H_2O_2, NaClO, NO) to investigate the selectivity of the probe **TCF-NBD** towards Cys/Hcy and GSH. As shown in **Fig. 4** and **S3**, the fluorescence intensity of probe **TCF-NBD** at 547 nm and 610 nm are significantly enhanced after the addition of 100 μM Cys or Hcy; and the fluorescence turn-on response only at 610 nm after addition of 100 μM GSH. However, there was no obvious change in fluorescence response can be observed when the probe reacted with other analytes with the excitation at 470 nm or 570 nm. These results indicated that the ability of **TCF-NBD** to specifically recognize Cys/Hcy and GSH over others relative analytes in complexed biosystem.

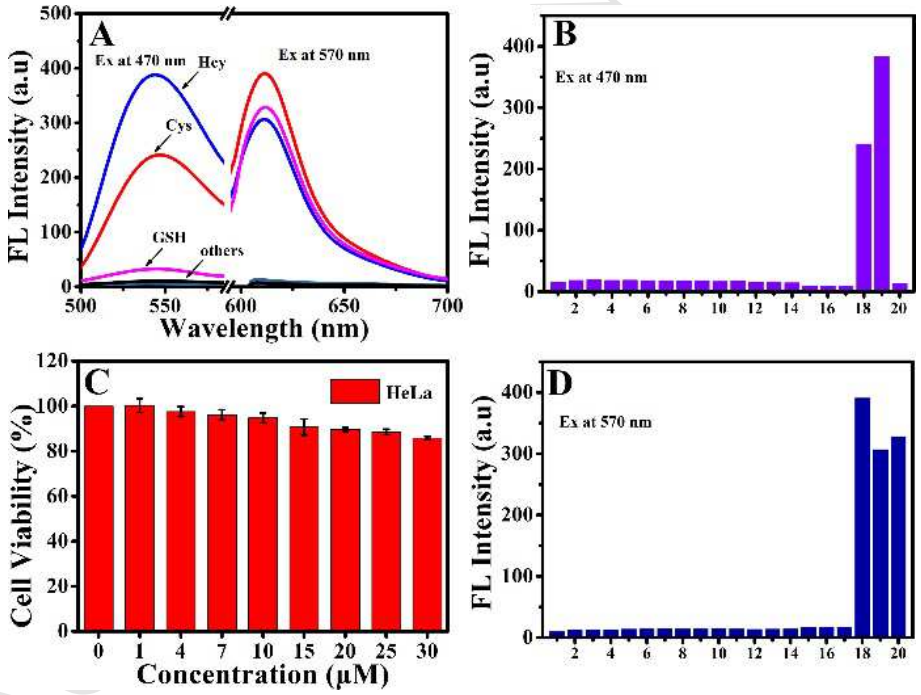

Fig. 4 (A) Fluorescence spectra of **TCF-NBD** (10 μM) in the presence of Cys, Hcy or GSH (100 μM) and some relevant species (500 μM): (1) Probe, (2) His, (3) Asp, (4) Val, (5) Phe, (6) Tyr, (7) Ala, (8) Ser, (9) Leu, (10) Arg, (11)Pro, (12)Thr, (13)Trp, (14)Lys, (15) H_2O_2, (16) NaClO, (17) NO, (18) Cys, (19) Hcy, (20) GSH in PBS (10 mM, pH 7.4, 10% DMF). Fluorescence intensity of **TCF-NBD** (10 μM) upon addition

of different analytes: (B) λ_{ex} =470 nm, λ_{em} =547 nm (D) λ_{ex} =570 nm, λ_{em} =610 nm. (C) The cell cytotoxicity of various concentration of **TCF-NBD** in HeLa cells for 24 h.

3.5. Fluorescence imaging of probe TCF-NBD in living cells

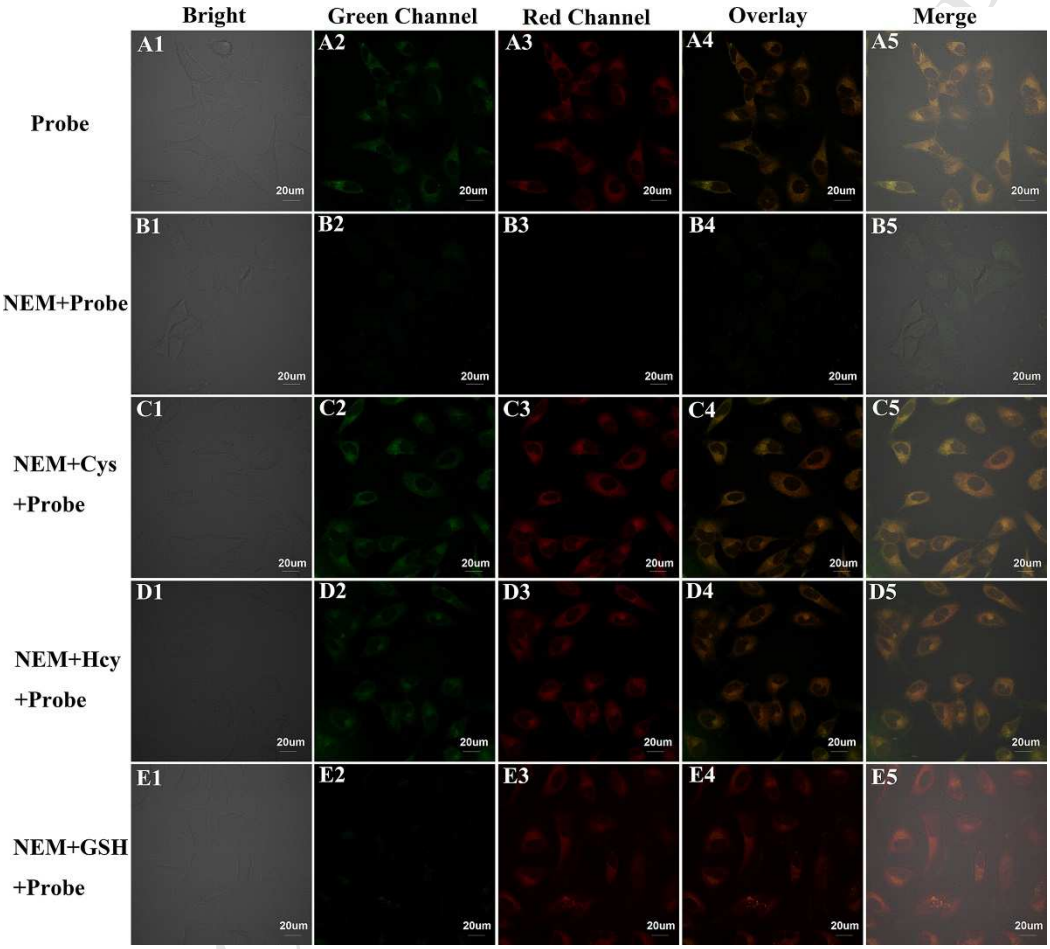

Fig.5 Fluorescence imaging for HeLa cells. (A1-A5): HeLa cells were incubated with 10 μM **TCF-NBD** only for 30 min; (B1-B5): The cells were pretreated with 500 μM NEM for 30 min, and then incubated with 10 μM **TCF-NBD** for 30 min. The cells were pretreated with 500 μM NEM for 30 min, and then treated with 100 μM Cys (C1-C5), Hcy (D1-D5) and GSH (E1-E5) respectively and further incubated with 10 μM **TCF-NBD** for 30 min. Green channel: λ_{ex} =488 nm, collected: 500-550 nm; Red

channel: λ_{ex} =559 nm, collected: 570-630 nm. Scaler bar: 20 μm.

In order to verify the bioavailability of the probe **TCF-NBD**, we evaluated its capability to selectively visualize intracellular Cys/Hcy and GSH with fluorescence imaging. Accordingly, the cytotoxicity of **TCF-NBD** was established using MTT assays with HeLa cells. It was found that the cell viabilities exceed 94% when incubated cells for 24 h with10 μM **TCF-NBD**, demonstrating that the probe **TCF-NBD** is of low cytotoxicity and is suitable for fluorescence confocal biological imaging (**Fig. 4C**).

As shown in **Fig. 5A**, when the HeLa cells were only incubated with probe **TCF-NBD** (10 μM), it shows fluorescence signals in green and red channels simultaneously, which were caused by the endogenous biothiols in HeLa cells. We then performed a series of control experiments so that to evaluate selective responses of probe **TCF-NBD** toward Cys/Hcy and GSH in living cells. When N-ethylmaleimide (NEM, a thiol-consumptive agent)-pretreated cells were further incubated with **TCF-NBD** for 30 min, however, an obvious fluorescence reduction in both green and red channels can be observed (**Fig. 5B**), indicating that thiols were completely reacted with NEM [68]. In contrast, when NEM-pretreated HeLa cells were incubated with Cys/Hcy and then treated with probe **TCF-NBD** for 30 min, strong fluorescence signals occurred in green and red channels (**Figs. 5C and 5D**). Upon the addition of 100 μM GSH to NEM-pretreated cells followed by incubation with probe, only obvious red fluorescence signal was observed (**Fig. 5E**). These above experiments indicated that **TCF-NBD** could discriminate intracellular Cys/Hcy

and GSH by different emission signals and serve as a potential tool for investigating the metabolism and mechanism of biothiols.

3.6. Fluorescence imaging of probe TCF-NBD in *Daphnia magna*

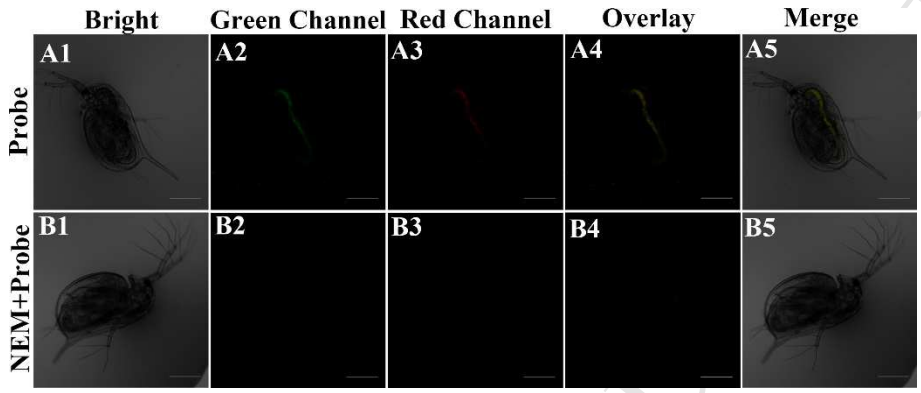

Fig.6 Fluorescence images of endogenous biothiols in *Daphnia magna*. (A1-A5) *Daphnia magna* were incubated with 10 μM **TCF-NBD** only for 30 min. (B1-B5) *Daphnia magna* were pretreated with 500 μM NEM for 30 min, and then incubated with 10 μM **TCF-NBD** for 30 min. Scale bar: 300 μm.

The ability of **TCF-NBD** for visualizing biothiols in vivo was also evaluated in living *Daphnia magna*, a widely used animal as a standard Environmental Protection Agency test organism [69], using fluorescence imaging. As shown in **Fig. 6A**, the gut of *Daphnia magna* exhibited strong fluorescence signals in green channel and red channel when the *Daphnia magna* were incubated with 10 μM **TCF-NBD** for 30 min, indicating that there were abundant endogenous biothiols in the gut of *Daphnia magna*. To verify this result, *Daphnia magna* were pretreated with 500 μM NEM for 30 min, and then incubated with 10 μM **TCF-NBD** for further 30 min before fluorescence imaging. The *Daphnia magna* displays almost unobservable

fluorescence signals in two channels (**Fig. 6B**), suggesting the signals observed in **Fig. 6A** were induced by endogenous biothiols. These results indicating that **TCF-NBD** could be used for tracking biothiols in complex living bodies.

4. Conclusions

In summary, an efficient fluorescent probe, **TCF-NBD**, for simultaneously discriminating Cys/Hcy and GSH by separated emissions via independent excitations was designed and synthesized. The strategy is to couple two fluorophores, **TCF-OH** and **NBD** with a biothiol-sensitive ether linkage. This probe emits a dual emission signal toward Cys and Hcy through a substitution- rearrangement cascade reaction; however, a single emission response toward GSH, which can be used to simultaneously distinguish Cys/Hcy and GSH. Taking the merits of low cytotoxicity and good selectivity of probe **TCF-NBD** into consideration, we have successfully applied it for discriminative detecting of Cys/Hcy and GSH in HeLa cells through fluorescence confocal imaging. More importantly, the in vivo ability of **TCF-NBD** was proved by the visualization of endogenous biothiols in *Daphnia magna*. Therefore, the probe **TCF-NBD** would serve as a powerful tool for further elucidating the physiological role of biothiols and conducting pathological analysis of thiol-related diseases.

Acknowledgements

This work was financially supported by National Science Foundation of China

(21576037, 21676047, 21421005, 21703025), NSFC-Liaoning United Fund (U1608222).

References

[1] Ball RO, Courtney-Martin G, Pencharz PB. The in vivo sparing of methionine by cysteine in sulfur amino acid requirements in animal models and adult humans. J Nutr 2006; 136: 1682S-1693S.

[2] Zhou Y, Yoon J. Recent progress in fluorescent and colorimetric chemosensors for detection of amino acids. Chem Soc Rev 2012; 41: 52-67.

[3] Townsend DM, Tew KD, Tapiero H. The importance of glutathione in human disease. Biomed Pharmacother 2003; 57: 145-155.

[4] Paul BD, Sbodio JI, Xu R, Vandiver MS, Cha JY, Snowman AM, et al. Cystathionine gamma-lyase deficiency mediates neurodegeneration in Huntington's disease. Nature 2014; 509: 96-100.

[5] Forman HJ, Zhang H, Rinna A. Glutathione: Overview of its protective roles, measurement, and biosynthesis. Mol Aspects Med 2009; 30: 1-12.

[6] Shahrokhian S. Lead phthalocyanine as a selective carrier for preparation of a cysteine-selective electrode. Anal Chem 2001; 73: 5972-5978.

[7] Refsum H, Smith AD, Ueland PM, Nexo E, Clarke R, McPartlin J, et al. Facts and recommendations about total homocysteine determinations: An expert opinion. Clin Chem 2004; 50: 3-32.

[8] Lu SC. Regulation of glutathione synthesis. Mol Aspects Med 2009; 30: 42-59.

[9] Seshadri S, Beiser A, Selhub J, Jacques PF, Rosenberg IH, D'Agostino RB, et al. Plasma homocysteine as a risk factor for dementia and Alzheimer's disease. New Engl J Med 2002; 346: 476-483.

[10] Chan J, Dodani SC, Chang CJ. Reaction-based small-molecule fluorescent probes for chemoselective bioimaging. Nat Chem 2012; 4: 973-984.

[11] Chen X, Wang F, Hyun JY, Wei T, Qiang J, Ren X, et al. Recent progress in the development of fluorescent, luminescent and colorimetric probes for detection of reactive oxygen and nitrogen species. Chem Soc Rev 2016; 45: 2976-3016.

[12] Jiao X, Li Y, Niu J, Xie X, Wang X, Tang B. Small-Molecule Fluorescent Probes for Imaging and Detection of Reactive Oxygen, Nitrogen, and Sulfur Species in Biological Systems. Anal Chem 2018; 90: 533-555.

[13] Yin C-X, Xiong K-M, Huo F-J, Salamanca JC, Strongin RM. Fluorescent Probes with Multiple Binding Sites for the Discrimination of Cys, Hcy, and GSH. Angew Chem Int Edit 2017; 56: 13188-13198.

[14] Zhang W, Huo F, Yin C. Recent advances of dicyano-based materials in biology and medicine. J Mater Chem B 2018; 6: 6919-6929.

[15] Lou Z, Li P, Han K. Redox-Responsive Fluorescent Probes with Different Design Strategies. Acc Chem Res 2015; 48: 1358-1368.

[16] Chen X, Zhou Y, Peng X, Yoon J. Fluorescent and colorimetric probes for detection of thiols. Chem Soc Rev 2010; 39: 2120-2135.

[17] Yang Y, Zhao Q, Feng W, Li F. Luminescent Chemodosimeters for Bioimaging. Chem Rev 2013; 113: 192-270.

[18] Yang M, Fan J, Zhang J, Du J, Peng X. Visualization of methylglyoxal in living cells and diabetic mice model with a 1,8-naphthalimide-based two-photon fluorescent probe. Chem Sci 2018; 9: 6758-6764.

[19] Li X, Huo F, Yue Y, Zhang Y, Yin C. A coumarin-based "off-on" sensor for fluorescence selectivily discriminating GSH from Cys/Hcy and its bioimaging in living cells. Sensor Actuat B-chem 2017; 253: 42-49.

[20] Liu T, Huo F, Li J, Chao J, Zhang Y, Yin C. An off-on fluorescent probe for specifically detecting cysteine and its application in bioimaging. Sensor Actuat B-chem 2016; 237: 127-132.

[21] Yue Y, Huo F, Li X, Wen Y, Yi T, Salamanca J, et al. pH-Dependent Fluorescent Probe That Can Be Tuned for Cysteine or Homocysteine. Org Lett 2017; 19: 82-85.

[22] Yue Y, Yin C, Huo F, Chao J, Zhang Y. Thiol-chromene click chemistry: A turn-on fluorescent probe for specific detection of cysteine and its application in bioimaging. Sensor Actuat B-chem 2016; 223: 496-500.

[23] Yang Y, Huo F, Yin C, Chao J, Zhang Y. An 'OFF-ON' fluorescent probe for specially recognize on Cys and its application in bioimaging. Dyes Pigments 2015; 114: 105-109.

[24] Huo F, Kang J, Yin C, Zhang Y, Chao J. A turn-on green fluorescent thiol probe based on the 1,2-addition reaction and its application for bioimaging. Sensor Actuat B-chem 2015; 207: 139-143.

[25] Yue Y, Huo F, Yue P, Meng X, Salamanca JC, Escobedo JO, et al. In Situ Lysosomal Cysteine-Specific Targeting and Imaging during Dexamethasone-Induced Apoptosis. Anal Chem 2018; 90: 7018-7024.

[26] Liu T, Huo FJ, Yin CX, Li JF, Niu LX. A highly selective fluorescence sensor for cysteine/homocysteine and its application in bioimaging. Rsc Advances 2015; 5: 28713-28716.

[27] Huo F-J, Sun Y-Q, Su J, Chao J-B, Zhi H-J, Yin C-X. Colorimetric Detection of

Thiols Using a Chromene Molecule. Org Lett 2009; 11: 4918-4921.

[28] Yang Y, Huo F, Yin C, Zheng A, Chao J, Li Y, et al. Thiol-chromene click chemistry: A coumarin-based derivative and its use as regenerable thiol probe and in bioimaging applications. Biosens Bioelectron 2013; 47: 300-306.

[29] Kang J, Huo F, Chao J, Yin C. Nitroolefin-based BODIPY as a novel water-soluble ratiometric fluorescent probe for detection of endogenous thiols. Spectrochim Acta A 2018; 195: 16-20.

[30] Xie XX, Yin CX, Yue YK, Huo FJ. Rational design of fluorescent probe for Cys dynamics imaging in living cell. Sensor Actuat B-chem 2018; 267: 76-82.

[31] Li J, Yue Y, Huo F, Yin C. Rational design of cysteine-specific ratiometric probe based on steric hindrance effect and its biological application. Dyes Pigments 2019; 164: 335-340.

[32] Chen T, Pei X, Yue Y, Huo F, Yin C. An enhanced fluorescence sensor for specific detection Cys over Hcy/GSH and its bioimaging in living cells. Spectrochim Acta A 2019; 209: 223-227.

[33] Peng H, Chen W, Cheng Y, Hakuna L, Strongin R, Wang B. Thiol Reactive Probes and Chemosensors. Sensors 2012; 12: 15907-15946.

[34] Yin C, Huo F, Zhang J, Martinez-Manez R, Yang Y, Lv H, et al. Thiol-addition reactions and their applications in thiol recognition. Chem Soc Rev 2013; 42: 6032-6059.

[35] Lin VS, Chen W, Xian M, Chang CJ. Chemical probes for molecular imaging and detection of hydrogen sulfide and reactive sulfur species in biological systems. Chem Soc Rev 2015; 44: 4596-4618.

[36] Sun W, Guo S, Hu C, Fan J, Peng X. Recent Development of Chemosensors Based on Cyanine Platforms. Chem Rev 2016; 116: 7768-7817.

[37] Niu L-Y, Chen Y-Z, Zheng H-R, Wu L-Z, Tung C-H, Yang Q-Z. Design strategies of fluorescent probes for selective detection among biothiols. Chem Soc Rev 2015; 44: 6143-6160.

[38] Liu T, Huo F, Yin C, Li J, Chao J, Zhang Y. A triphenylamine as a fluorophore and maleimide as a bonding group selective turn-on fluorescent imaging probe for thiols. Dyes Pigments 2016; 128: 209-214.

[39] Kong F, Liu R, Chu R, Wang X, Xu K, Tang B. A highly sensitive near-infrared fluorescent probe for cysteine and homocysteine in living cells. Chem Commun 2013; 49: 9176-9178.

[40] Zhang J, Ji X, Ren H, Zhou J, Chen Z, Dong X, et al. Meso-heteroaryl BODIPY dyes as dual-responsive fluorescent probes for discrimination of Cys from Hcy and GSH. Sensor Actuat B-chem 2018; 260: 861-869.

[41] Lee D, Jeong K, Luo X, Kim G, Yang Y, Chen X, et al. Near-infrared fluorescent probes for the detection of glutathione and their application in the fluorescence imaging of living cells and tumor-bearing mice. J Mater Chem B 2018; 6: 2541-2546.

[42] Wang J-Y, Liu Z-R, Ren M, Kong X, Lin W. A fast-response two-photon fluorescent probe for the detection of Cys over GSH/Hcy with a large turn-on signal and its application in living tissues. J Mater Chem B 2017; 5: 134-138.

[43] Yue Y, Huo F, Ning P, Zhang Y, Chao J, Meng X, et al. Dual-Site Fluorescent Probe for Visualizing the Metabolism of Cys in Living Cells. J Am Chem Soc 2017; 139: 3181-3185.

[44] Fu Y-J, Li Z, Li C-Y, Li Y-F, Wu P, Wen Z-H. Borondipyrrolemethene-based fluorescent probe for distinguishing cysteine from biological thiols and its application in cell image. Dyes Pigments 2017; 139: 381-387.

[45] Li M, Cui P, Li K, Feng J, Zou M, Yu X. Dual-site fluorescent probe for highly selective and sensitive detection of sulfite and biothiols. Chinese Chem Lett 2018; 29: 992-994.

[46] He L, Yang X, Xu K, Lin W. Improved Aromatic Substitution Rearrangement-Based Ratiometric Fluorescent Cysteine-Specific Probe and Its Application of Real-Time Imaging under Oxidative Stress in Living Zebrafish. Anal Chem 2017; 89: 9567-9573.

[47] Huang Y, Zhou Q, Feng Y, Zhang W, Fang G, Fang M, et al. Rational design of a ratiometric two-photon fluorescent probe for real-time visualization of apoptosis. Chem Commun 2018; 54: 10495-10498.

[48] Gao M, Wang R, Yu F, Li B, Chen L. Imaging of intracellular sulfane sulfur expression changes under hypoxic stress via a selenium-containing near-infrared fluorescent probe. J Mater Chem B 2018; 6: 6637-6645.

[49] Wang F-F, Liu Y-J, Wang B-B, Gao L-X, Jiang F-L, Liu Y. A BODIPY-basedmitochondria-targeted turn-on fluorescent probe with dual response units for the rapid detection of intracellular biothiols. Dyes Pigments 2018; 152: 29-35.

[50] Han C, Yang H, Chen M, Su Q, Feng W, Li F. Mitochondria-Targeted Near-Infrared Fluorescent Off-On Probe for Selective Detection of Cysteine in

Living Cells and in Vivo. ACS Appl Mater Inter 2015; 7: 27968-27975.

[51] Yin K, Yu F, Zhang W, Chen L. A near-infrared ratiometric fluorescent probe for cysteine detection over glutathione indicating mitochondrial oxidative stress in vivo. Biosens Bioelectron 2015; 74: 156-164.

[52] Niu W, Guo L, Li Y, Shuang S, Dong C, Wong MS. Highly Selective Two-Photon Fluorescent Probe for Ratiometric Sensing and Imaging Cysteine in Mitochondria. Anal Chem 2016; 88: 1908-1914.

[53] Yang L, Su Y, Geng Y, Zhang Y, Ren X, He L, et al. A Triple-Emission Fluorescent Probe for Discriminatory Detection of Cysteine/Homocysteine, Glutathione/Hydrogen Sulfide, and Thiophenol in Living Cells. ACS Sensors 2018; 3: 1863-1869.

[54] Yin G-x, Niu T-t, Gan Y-b, Yu T, Yin P, Chen H-m, et al. A Multi-signal Fluorescent Probe with Multiple Binding Sites for Simultaneous Sensing of Cysteine, Homocysteine, and Glutathione. Angew Chem Int Edit 2018; 57: 4991-4994.

[55] Zhang H, Liu R, Liu J, Li L, Wang P, Yao SQ, et al. A minimalist fluorescent probe for differentiating Cys, Hcy and GSH in live cells. Chem Sci 2016; 7: 256-260.

[56] Tian Y, Zhu B, Yang W, Jing J, Zhang X. A fluorescent probe for differentiating Cys, Hcy and GSH via a stepwise interaction. Sensor Actuat B-chem 2018; 262: 345-349.

[57] Hwang C, Sinskey AJ, Lodish HF. Oxidized redox state of glutathione in the

493 endoplasmic reticulum. Science 1992; 257: 1496-1502.

494 [58] Jung HS, Pradhan T, Han JH, Heo KJ, Lee JH, Kang C, et al. Molecular
495 modulated cysteine-selective fluorescent probe. Biomaterials 2012; 33:
496 8495-8502.

497 [59] Lu Z, Fan W, Shi X, Lu Y, Fan C. Two Distinctly Separated Emission
498 Colorimetric NIR Fluorescent Probe for Fast Hydrazine Detection in Living
499 Cells and Mice upon Independent Excitations. Anal Chem 2017; 89: 9918-9925.

500 [60] Wang X, Guo Z, Zhu S, Tian H, Zhu W. A naked-eye and ratiometric
501 near-infrared probe for palladium via modulation of a pi-conjugated system of
502 cyanines. Chem Commun 2014; 50: 13525-13528.

503 [61] Wang K, Zhao C-X, Leng T-H, Wang C-Y, Lu Y-X, Shen Y-J, et al. Dual
504 quenching strategy for sensitive detection of toxic thiolphenols based on a
505 NIR-illuminant platform with a large Stokes shift. Dyes Pigments 2018; 151:
506 194-201.

507 [62] Hu Q, Yu C, Xia X, Zeng F, Wu S. A fluorescent probe for simultaneous
508 discrimination of GSH and Cys/Hcy in human serum samples via
509 distinctly-separated emissions with independent excitations. Biosens Bioelectron
510 2016; 81: 341-348.

511 [63] Wang P, Wang Y, Li N, Huang J, Wang Q, Gu Y. A novel DCM-NBD conjugate
512 fluorescent probe for discrimination of Cys/Hcy from GSH and its bioimaging
513 applications in living cells and animals. Sensor Actuat B-chem 2017; 245:
514 297-304.

515 [64] Montoya LA, Pluth MD. Hydrogen Sulfide Deactivates Common
516 Nitrobenzofurazan-Based Fluorescent Thiol Labeling Reagents. Anal Chem
517 2014; 86: 6032-6039.
518 [65] Gao X, Li X, Li L, Zhou J, Ma H. A simple fluorescent off-on probe for the
519 discrimination of cysteine from glutathione. Chem Commun 2015; 51:
520 9388-9390.
521 [66] Hammers MD, Pluth MD. Ratiometric Measurement of Hydrogen Sulfide and
522 Cysteine/Homocysteine Ratios Using a Dual-Fluorophore Fragmentation
523 Strategy. Anal Chem 2014; 86: 7135-7140.
524 [67] Lee D, Kim G, Yin J, Yoon J. An aryl-thioether substituted nitrobenzothiadiazole
525 probe for the selective detection of cysteine and homocysteine. Chem Commun
526 2015; 51: 6518-6520.
527 [68] Yellaturu CR, Bhanoori M, Neeli I, Rao GN. N-ethylmaleimide inhibits
528 platelet-derived growth factor BB-stimulated Akt phosphorylation via activation
529 of protein phosphatase 2A. J Biol Chem 2002; 277: 40148-40155.
530 [69] Lovern SB, Klaper R. Daphnia magna mortality when exposed to titanium
531 dioxide and fullerene (C-60) nanoparticles. Environ Toxicol Chem 2006; 25:
532 1132-1137.

Supporting Information

Simultaneous visualization of cysteine/homocysteine and glutathione in living cells and *Daphnia magna* via dual-signaling fluorescent chemosensor

Mingwang Yang[1], Jiangli Fan*[1,2], Wen Sun[1,2], Jianjun Du[1,2], Saran Long[1,2], Xiaojun Peng[1,2]

[1]State Key Laboratory of Fine Chemicals, Dalian University of Technology, 2 Linggong Road, Dalian, 116024, P.R. China.

[2]Research Institute of Dalian University of Technology in Shenzhen, Gaoxin South fourth Road, Nanshan District, Shenzhen 518057, China

Email: fanjl@dlut.edu.cn

Table S1 Comparison of fluorescent probes for the selective detection of biothiols

Probes	Reaction time	Test system	Selectivity	Two signals	Detection limit	Biological system
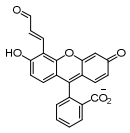 *Chem. Commun.*, 2010, **46**, 5707-5709.	120 min	PBS	Cys	No	Cys 39 μM	No application
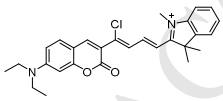 *Anal.Chem.*, DOI: 10.1021/acs.analchem.8b04485.	60 min	PBS/EtOH =4:1	Cys/Hcy+ GSH	No	Cys 2.96 μM Hcy 6.14 μM GSH 6.84 μM	HepG-2 cells
 *Chem. Sci.*, 2016, **7**,	120 min	PBS+CATB	Cys/Hcy+ GSH	No	Cys 0.02 μM Hcy 2.27 μM GSH 0.24 μM	HeLa cells

256-260.						
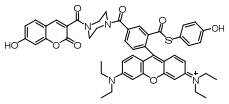 *Chem. Eur. J.*, 2012, **18**, 14520 – 14526.	Cys: 12 min Hcy: 20min	PBS/DMF =9:1	Cys+Hcy	No	Cys 0.64 μM Hcy 3.6 nM	BEL□7402 cells
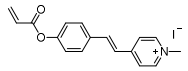 *Anal. Chem.*, 2016, **88**, 1908−1914.	6 min	PBS/DMSO =1:1	Cys	No	Not mentioned	HeLa cells
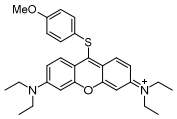 *Chem. Sci.*, 2014, **5**, 3183–3188.	Cys/Hcy:10 min GSH: 2 min	PBS	Cys/Hcy+ GSH	No	Not mentioned	B16 cells
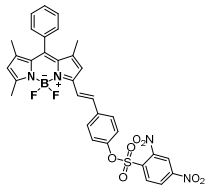 *Biosens. Bioelectron.*, 2011, **26**, 3012-3017.	20 min	MeOH/H_2O =4:1	Cys	No	Cys 7.2 μM	SGC-H446 cells
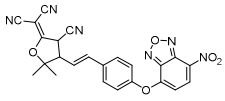 **This work**	about 4 min	PBS/DMF =9:1	Cys/Hcy+ GSH	Yes	Cys 0.015 μM Hcy 0.034 μM GSH 0.030 μM	HeLa cells, *Daphnia magna*

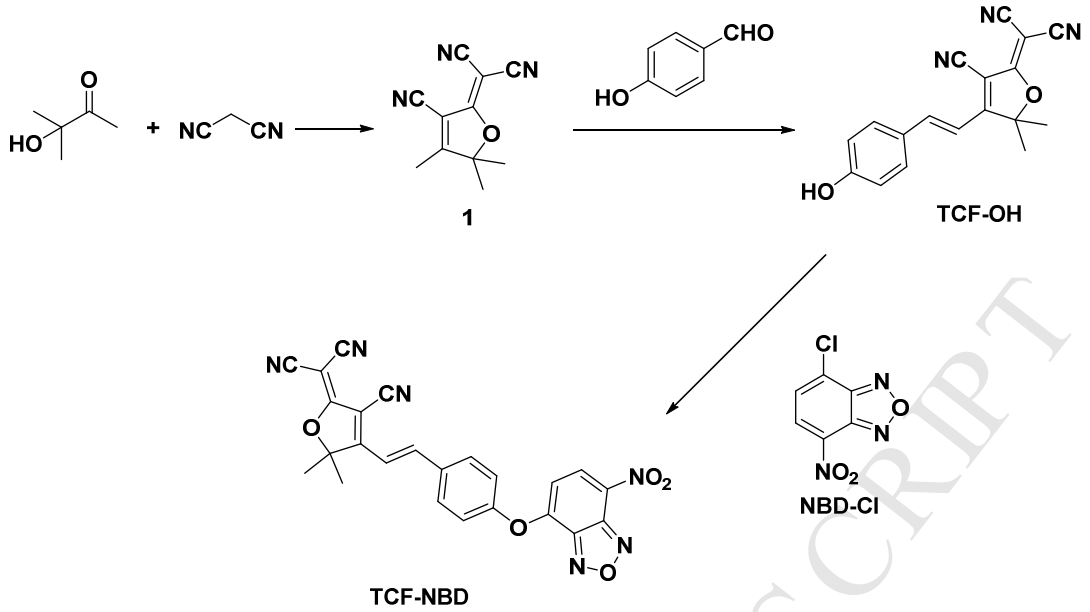

Scheme S1 Synthetic procedure of **TCF-NBD**

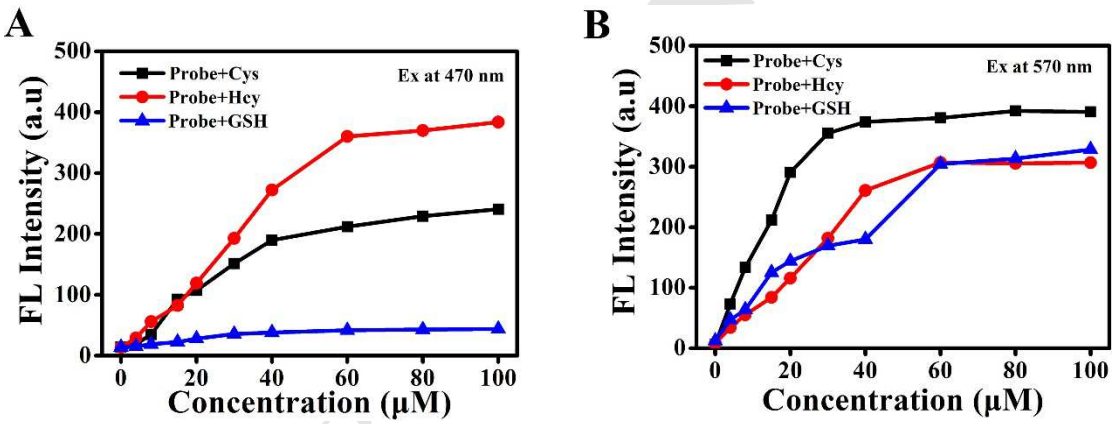

Figure S1 The fluorescence intensity changes of **TCF-NBD** at 547 nm (A) and 610 nm (B) in presence of different concentration analytes. The intensity at 547 and 610 nm was obtained with excitation at 470 nm and 570 nm, respectively.

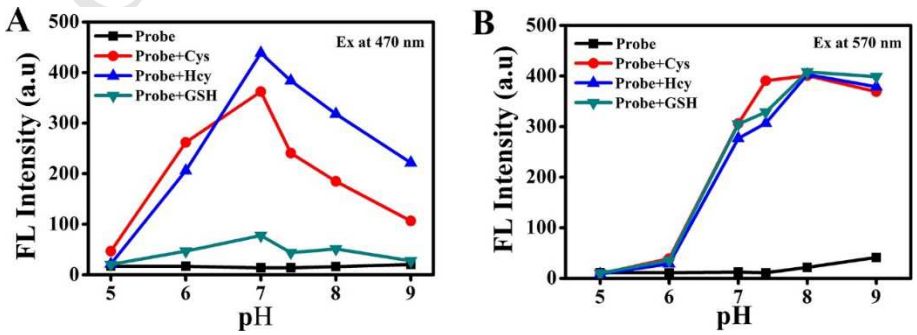

Figure S2 The fluorescence intensity of **TCF-NBD** (10 μM) at (A) 547 nm and (B)

610 nm in the presence or absence of 100 μM biothiols in various pH ranging from 4.0 to 10.0 PBS buffer (10 mM, pH 7.4, 10% DMF), respectively.

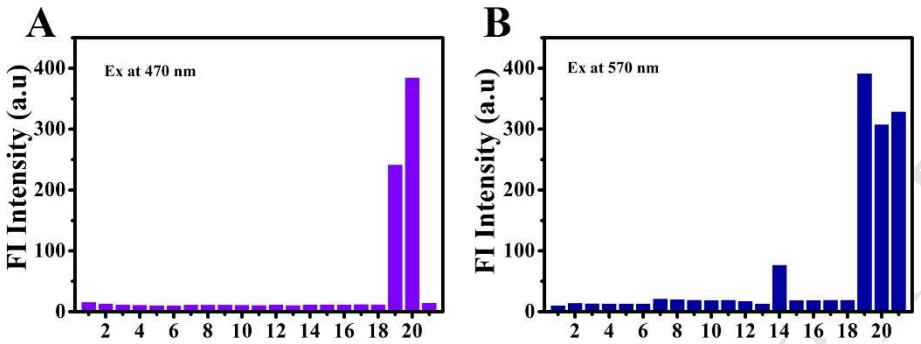

Figure S3 Fluorescence spectra of **TCF-NBD** (10 μM) in the presence of Cys, Hcy or GSH (100 μM) and some relevant species (500 μM): (1) Probe, (2) $NaHCO_3$, (3) $NaClO_4$, (4) NaOAc, (5) $AgNO_3$, (6) NaSCN, (7) $PdCl_2$, (8) $MgCl_2$, (9) NaF, (10) KBr, (11) KI, (12) Na_2SO_4, (13) Na_2SO_3, (14) Na_2S, (15) $FeCl_3$, (16) $CaCl_2$, (17) $ZnCl_2$, (18) $CuCl_2$, (19) Cys, (20) Hcy, (21) GSH in PBS (10 mM, pH 7.4, 10% DMF). Fluorescence intensity of **TCF-NBD** (10 μM) upon addition of different analytes: (A) λ_{ex} =470 nm, λ_{em} =547 nm (B) λ_{ex} =570 nm, λ_{em} =610 nm.

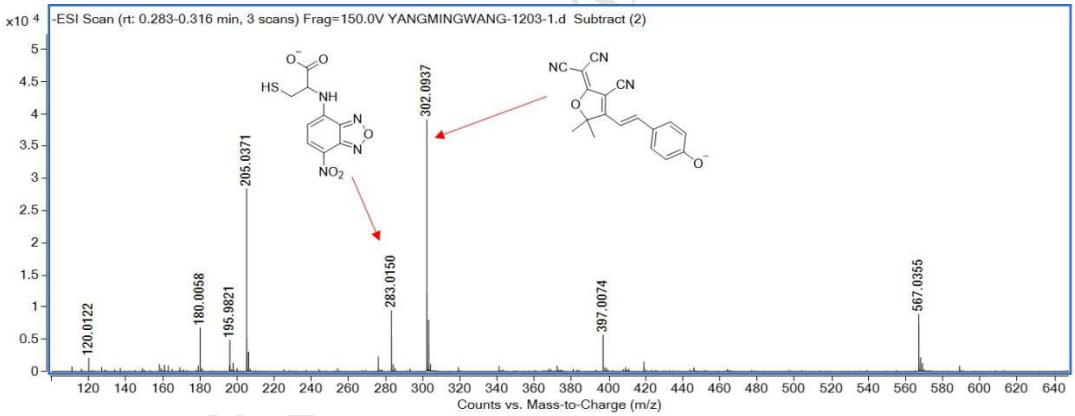

Figure S4 HRMS spectra of probe **TCF-NBD** treated with Cys.

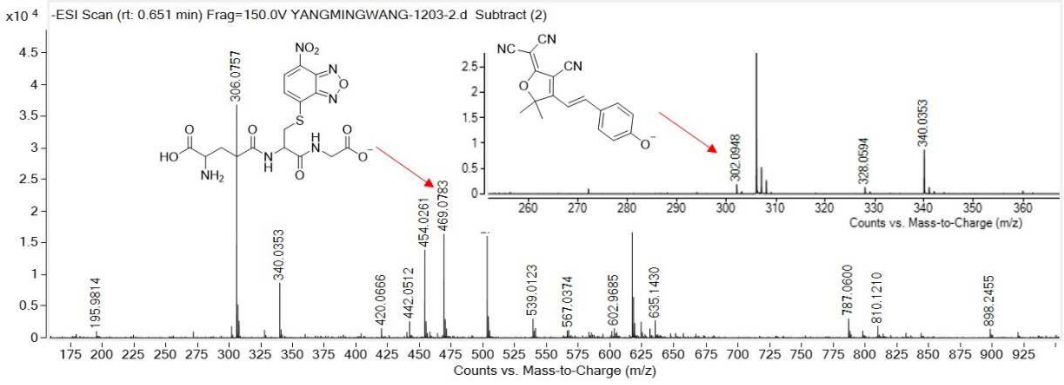

Figure S5 HRMS spectra of probe **TCF-NBD** treated with GSH.

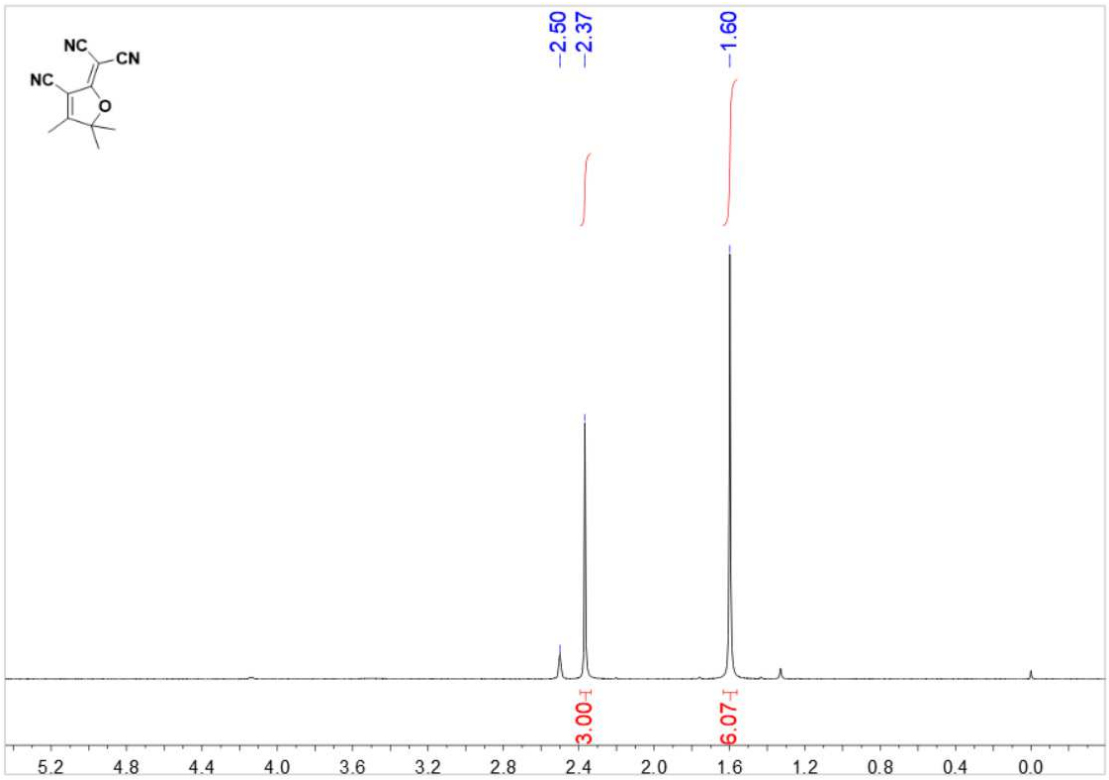

Figure S6 ^{1}H NMR of the compound **1** in DMSO-d_6

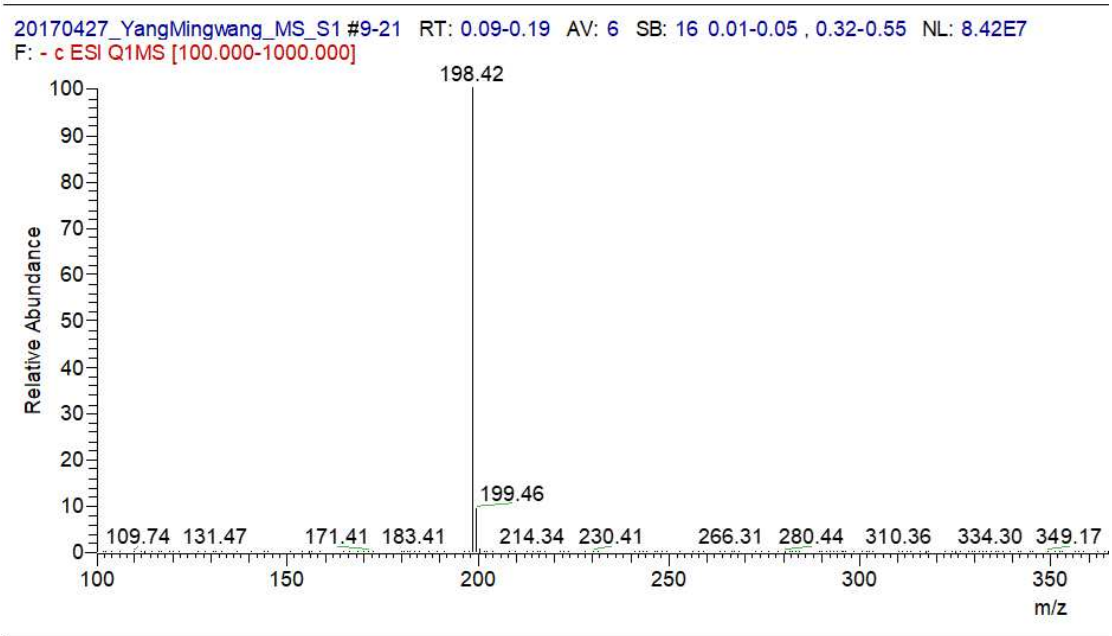

Figure S7 MS of probe compound **1**

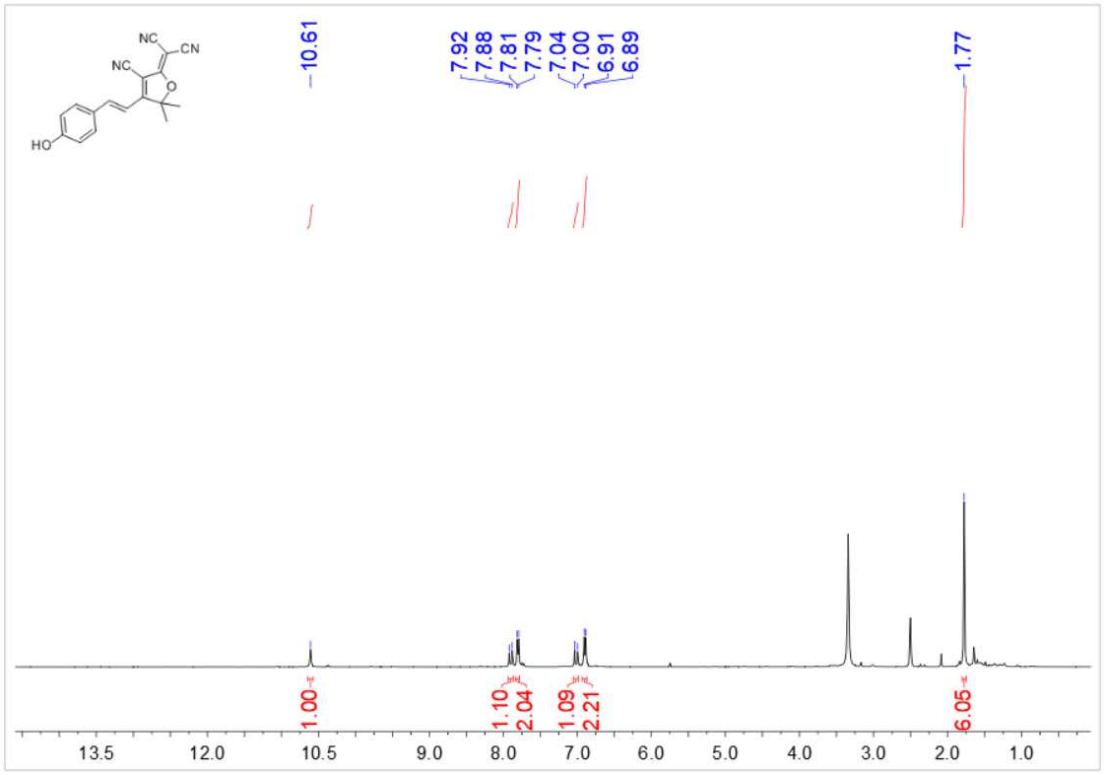

Figure S8 ^{1}H NMR of the **TCF-OH** in DMSO-d_6

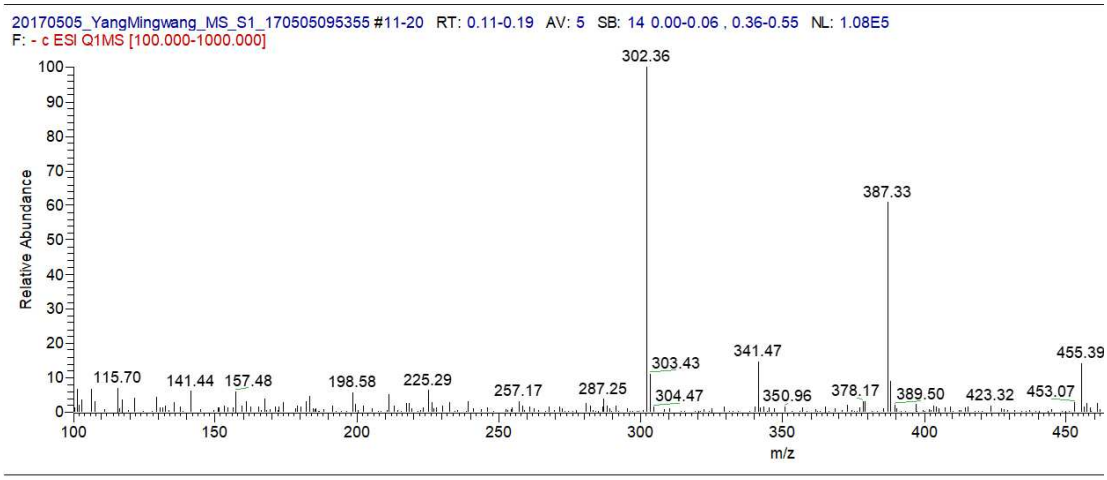

Figure S9 MS of probe **TCF-OH**

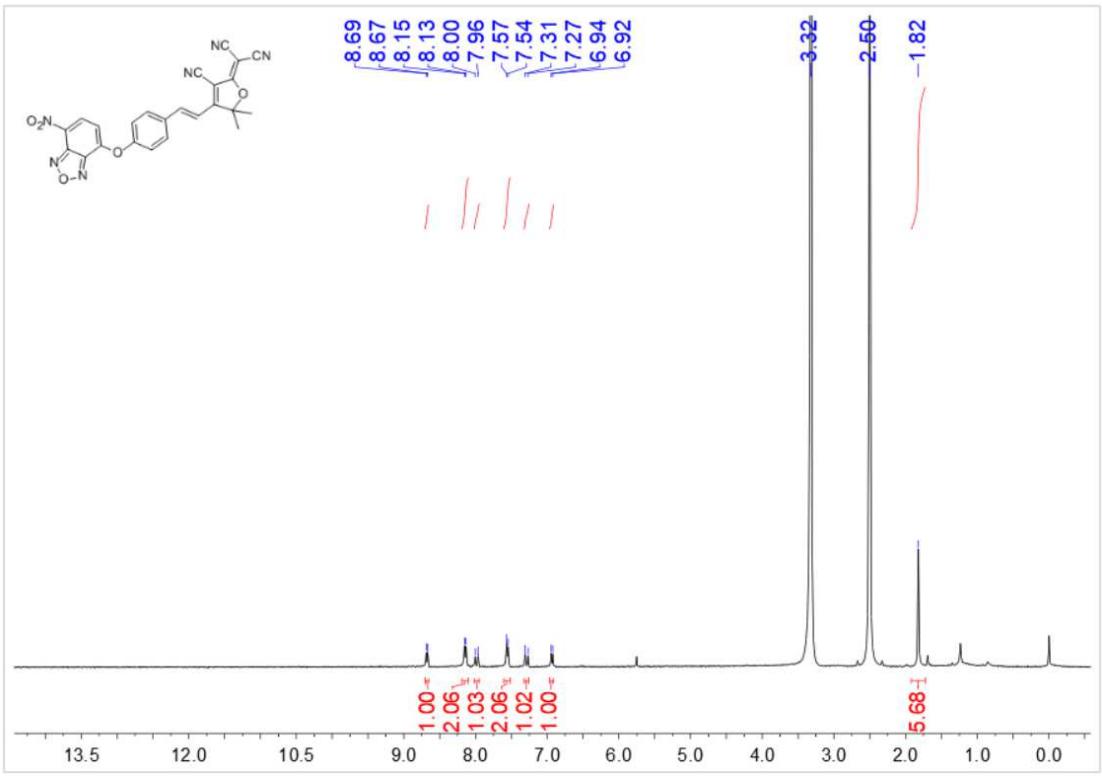

Figure S10 ^{1}H NMR of the **TCF-NBD** in DMSO-d_6

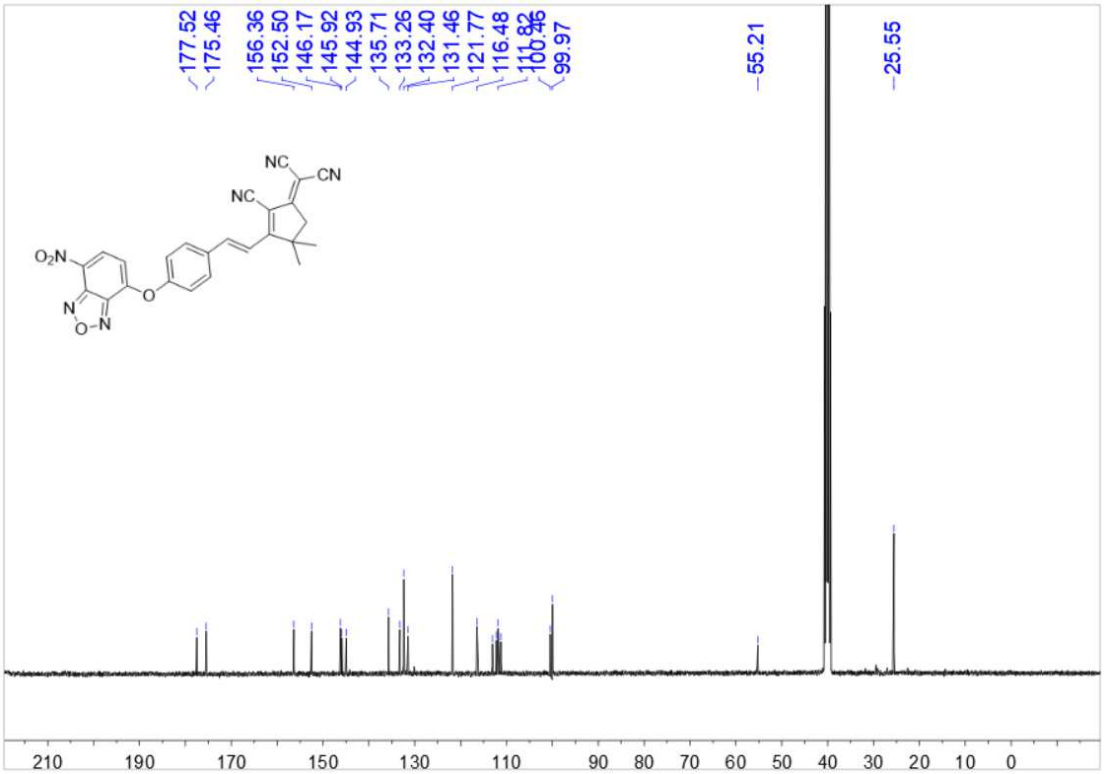

Figure S11 ^{13}C NMR of the **TCF-NBD** in DMSO-d_6

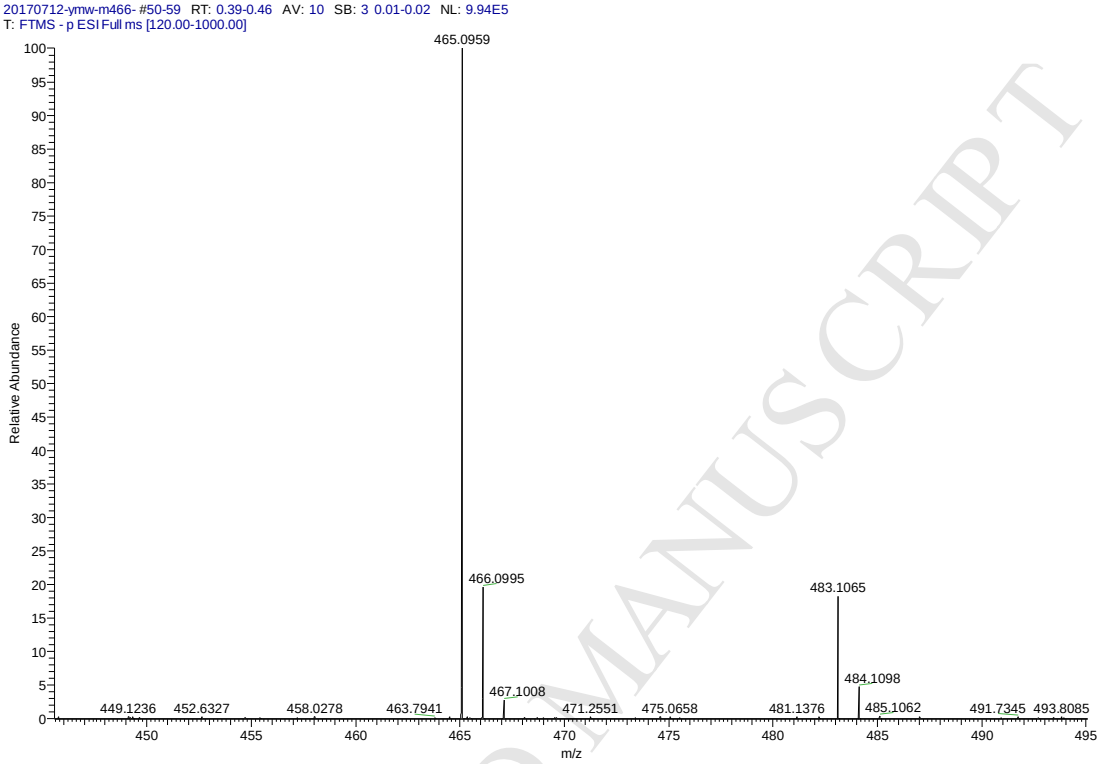

Figure S12 HRMS of probe **TCF-NBD**

Table S2 Detection limit of the analytes

Analyte	Regression curve equation	Detection limit (μM)
Cys	y=13.502x + 13.652, R^2=0.995	0.015
Hcy	y=5.937x + 4.684, R^2=0.988	0.034
GSH	y=6.672x + 15.822, R^2=0.985	0.030

Highlights

- A new fluorescent probe by combining a dicyanomethylenedifuran (TCF)-based fluorophore with 7-Nitrobenzofurazan (NBD) was developed.
- It exhibits two independent fluorescence signals with separated excitation, which was used to simultaneously distinguish Cys/Hcy and GSH.
- The probe displays selective and sensitive recognition towards biothiols with fast response time.
- The probe is low cytotoxicity and has been successfully applied to image intracellular Cys/Hcy and GSH in living HeLa cells and *Daphnia magna*.